Coherent wake emission spectroscopy as a probe of steep plasma density profiles

A. Malvache,[1,*] A. Borot,[1] F. Quéré,[2] and R. Lopez-Martens[1]
[1]*Laboratoire d'Optique Appliquée, ENSTA ParisTech, CNRS, Ecole Polytechnique, UMR 7639, 91761 Palaiseau, France*
[2]*CEA, IRAMIS, Service des Photons Atomes et Molécules, 91191 Gif/Yvette, France*
(Received 15 July 2012; published 15 March 2013)

Precise knowledge of the plasma density gradient created by an intense laser field at the surface of a solid is essential for understanding and controlling the resulting laser-plasma interaction. We present a novel experimental method for determining the scale length of such a gradient in a single shot, based on the spectral analysis of coherent wake emission by a laser-induced solid density plasma, using an analytical model of this emission process. We illustrate this approach in a pump-probe experiment, where it is used to measure the expansion velocity of a plasma into a vacuum.

DOI: 10.1103/PhysRevE.87.035101 PACS number(s): 52.38.Kd, 42.65.Ky

When an intense ($I \gtrsim 10^{15}$ W cm^{-2}) femtosecond laser pulse interacts with a solid, a thin layer of plasma is formed at the target surface, with an electronic density close to that of the solid itself ($\approx 10^{23}$ cm^{-3}), typically corresponding to several hundred times the critical density N_c for the laser frequency. Depending on the temporal contrast and peak intensity of the laser pulse, and on the nature of the solid, this plasma can be created either by the pulse itself during its rising edge or, some time before, by the so-called light pedestal surrounding the pulse. Whatever the case may be, plasma expansion toward the vacuum always occurs before the end of the pulse, such that the laser electric field couples to an electronic density profile that varies continuously from 0 to many times N_c. The scale length of this density gradient is known to have a major influence on the laser-plasma interaction, both qualitatively and quantitatively.

Qualitatively, it determines the transition between the different mechanisms of laser energy absorption by the plasma [1] and which mechanisms come into play for harmonic generation in the reflected laser beam [2,3]. Quantitatively, depending on the amount of energy effectively absorbed by the plasma, it will affect the outcome of processes such as ion acceleration. The efficiency of high-harmonic generation is also sensitive to even small variations of this density gradient [3], on the scale of a few tens of nanometers only, i.e., a small fraction of the laser wavelength λ_L. This parameter will thus be a key player in the optimization of future attosecond light sources based on laser-induced plasmas.

Predicting or measuring this parameter remains, however, extremely challenging. Theoretically, this is because plasma formation depends not only on the ionization dynamics of the solid, but also on the temporal variation of laser intensity over a large dynamic range. As a result, despite their sophistication, plasma simulation codes cannot be fully predictive, especially in the case of targets such as wide-bandgap insulators (e.g., SiO_2), where adjustable parameters have to be used to account for the complex ionization processes [4].

Experimentally, the most effective method so far for determining short density gradients (i.e., $L \lesssim \lambda_L$) is time-resolved interferometry [5], which measures the phase shift induced by the plasma expansion on a reflected probe pulse. However, this approach becomes very challenging for very short density gradients ($L \ll \lambda_L$), especially at very high laser intensities and in single-shot mode [6,7].

In this article, we describe a new and simple scheme for accurately measuring density gradients at the surface of laser-induced overdense plasmas, with a sensitivity better than $\lambda_L/200$. This method exploits the spectral profile of the harmonic peaks generated in the reflected beam by the coherent wake emission (CWE) mechanism [3,8,9]. This harmonic emission can be induced either directly by the main laser pulse, which is responsible for the creation of the gradient, or by an independent probe pulse. We demonstrate both schemes experimentally.

For obliquely incident p-polarized laser light, and at moderate laser intensities, $a_0 = 0.1$–1 (where $a_0^2 = I\lambda_L^2/I_0$, with I the laser intensity and $I_0 = 1.37 \times 10^{18}$ W cm^{-2} μm^2), CWE is the dominating mechanism for harmonic generation in the reflected beam. It is based on the excitation of collective electron oscillations in the overdense (density $N > N_c$) part of the density gradient by sub-laser-cycle electron bunches. Within each laser field cycle, the laser electric field accelerates electrons from the critical surface out into vacuum and then back into the plasma layer [Fig. 1(a)]. These so-called Brunel electrons [11] form spatially localized electron density peaks of attosecond duration throughout the overdense plasma layer due to collective trajectory crossings [Fig. 1(a)]. High-frequency plasma oscillations are impulsively excited in the wake of this electron bunch.

In the inhomogeneous part of the plasma formed by the density gradient, these longitudinal plasma oscillation subsequently emit an attosecond XUV burst through linear-mode conversion into transverse electromagnetic modes, almost immediately after their excitation by Brunel electron bunching [12]. The broad XUV spectrum $A(\omega)$ of this attosecond pulse is made up of the frequencies $\omega_p(x)$ emitted at different depths x inside the plasma gradient, such that the local plasma frequency $\omega_p(x) = \sqrt{N(x)e^2/m\epsilon_0}$. Repeated over many laser cycles, this process leads to the emission of an attosecond pulse train (APT), whose spectrum consists in harmonics of the incident laser frequency. CWE thus occurs precisely within the plasma density gradient at the target surface and, therefore, constitutes a natural probe of this gradient [10]. We

*arnaud.malvache@ensta-paristech.fr

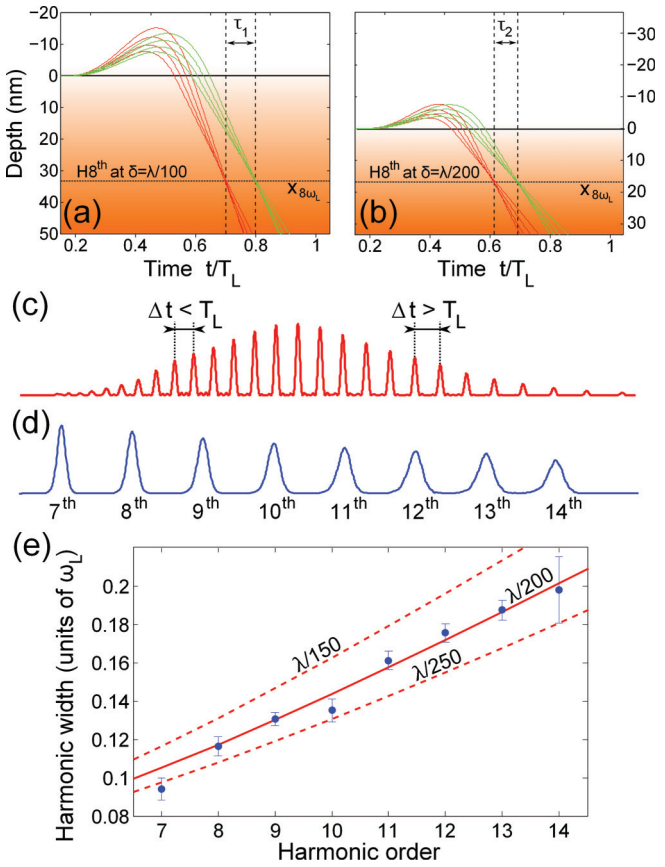

FIG. 1. (Color) (a, b) Brunel electron trajectories for $a_0 = 0.4$, for electrons crossing at a given depth $x_{8\omega_L}$ in the plasma, such that $\omega_p(x_{8\omega_L}) = 8\omega_L$, for two density gradients, (a) $\delta = \lambda_L/100$ and (b) $\delta = \lambda_L/200$. The shaded (red) area corresponds to the overdense part of the plasma ($N > N_c \cos^2\theta$). Red lines are the trajectories around the maximum of the laser pulse envelope, and green lines in its edges, at a time when the laser amplitude is halved. (c) Typical unevenly spaced CWE attosecond pulse train. (d) Corresponding harmonic spectrum from $7\,\omega_L$ to $14\,\omega_L$. (e) Harmonic spectral width as a function of harmonic order for $a_0 = 0.2$, from experiment [filled (blue) circles] and from the analytical model for different plasma density gradients [(red) lines].

first explain how the gradient scale length directly affects the spectral profile of individual CWE harmonics.

The instant of emission of the attosecond pulse within a given laser cycle is determined by the amount of time needed for Brunel electrons to travel up to the point of generation of XUV radiation [13]. This time decreases with increasing laser electric field amplitude [Fig. 1(a)] due to the higher velocities of returning Brunel electrons. As a result, attosecond pulses generated around the maximum of the laser pulse are emitted earlier in the laser cycle than those emitted at a lower intensity at the leading and trailing edges of the pulse. The time-varying intensity envelope $I(t)$ of the laser pulse therefore leads to the emission of an unevenly spaced APT [14,15] [Fig. 1(c)].

An attosecond pulse of central frequency ω generated by CWE is emitted at depth x_ω in the density gradient, such that the plasma frequency $\omega_p\,[N(x_\omega)] = \omega$. As a first approximation, the emission time t_e of this pulse corresponds to the Brunel electron trajectory crossing time t_c at this position x_ω [12]. Using the simple model initially proposed by Brunel [11] to calculate the electron trajectories, an analytical formula can be derived [16] for the crossing time $t_c(n)$ of Brunel electrons during the nth optical cycle of the laser field:

$$\frac{t_c(n)}{T_L} = n + \mu + \nu\left(\frac{x_\omega}{\lambda_L a_0 \sin\theta}\right)^{1/3}, \qquad (1)$$

where $\mu = 0.307$ and $\nu = 0.725$ are analytically calculated constants, $t/T_L = n$ corresponds to the 0 crossing of the laser E field in the nth optical period, and position x_ω is measured with respect to the reflection point of the laser, where $N = N_c \cos^2\theta$, with θ the laser angle of incidence on the target surface. This equation has been validated by comparison with particle-in-cell simulations [16] and was found to be very accurate, as long as $3 \times 10^{-3} < x_\omega/\lambda_L a_0 \sin\theta < 0.3$. Our model shows that this crossing time t_c is totally independent of the details of the plasma property [16], which is a crucial condition for the present measurement method: the Brunel electron bunches can be used as an invariant probe of the plasma, where they trigger the generation of harmonics, whose properties then depend on the plasma density profile.

As anticipated, Eq. (1) shows that t_c depends on the laser intensity $I \propto a_0^2$ and, therefore, varies in time with the laser pulse intensity envelope $I(t)$. It also explicitly depends on the distance x_ω and, consequently, on the plasma density profile. Qualitatively, this is because for sharper density gradients, returning Brunel electrons need to travel shorter distances inside the plasma before triggering CWE, and the attosecond pulse is thus emitted earlier within each laser optical cycle [compare Figs. 1(a) and 1(b)]. Information about the plasma density profile is therefore encoded in the temporal structure of the APT generated by CWE: a sharper density gradient reduces the difference in delay of emission due to cycle-to-cycle variation of the electric field amplitude across the laser pulse [$\tau_2 < \tau_1$ in Figs. 1(a) and 1(b)], leading to an APT with a smaller deviation from temporal periodicity.

Such temporal effects have a direct influence on the harmonic spectrum associated with the APT [13], which is straightforward to measure experimentally. Indeed, an uneven spacing of the pulses in the train leads to broader, frequency-chirped harmonics [Fig. 1(d)] because the central part of the APT (generated around the maximum of the laser pulse envelope) beats at the laser frequency ω_L, leading to a signal at $k\omega_L$ in the harmonic spectrum (k integer), while the head and tail of the APT beat at higher and lower frequencies, respectively, leading to detuned harmonic signals at $k(\omega_L - \epsilon)$ and $k(\omega_L + \epsilon)$ (where $\epsilon \ll \omega_L$). This spectral broadening effect increases with harmonic order [Fig. 1(d)] and gets less pronounced for smaller deviations from perfect periodicity of the APT. A sharper density gradient therefore results in narrower CWE harmonic peaks.

Mathematically, the CWE harmonic spectrum is written as

$$E(\omega) = \sum_n a(n) A(\omega) e^{i\omega t_e(n)}, \qquad (2)$$

where $a(n)$ and $t_e(n)$ are the amplitude and the emission time of the attosecond pulse generated in the nth laser cycle, respectively, and $A(\omega)$ is the spectral amplitude of individual

attosecond pulses. In the following, we combine this equation with Eq. (1) for the emission times $t_e(n) \approx t_c(n)$, in order to calculate theoretical CWE harmonic spectra as a function of x_ω. This requires knowledge of the $a(n)$ coefficients, which can be evaluated experimentally, as explained below. Individual harmonic spectral widths provided by this model exhibit a clear dependence on the plasma density profile, as the latter determines the point of emission x_ω and hence the values of $t_e(n)$.

Our approach thus consists in adjusting the distance x_ω in this model to fit the harmonic widths measured experimentally. This does not require any assumption about the shape of the density gradient. However, to enable a direct comparison with the existing literature, henceforth we assume an exponential profile, $N(x) = N_c \cos^2\theta \exp(x/\delta)$. The scale length δ can then be directly deduced from the retrieved distance x_ω using $\delta = x_\omega/2 \ln(\omega/\omega_L \cos\theta)$.

We now turn to the experimental demonstration of this approach for measuring δ. The experimental study is performed using the "Salle Noire" laser system at Laboratoire d'Optique Appliquée, delivering 30-fs, 2.5-mJ pulses at 800 nm and a 1-kHz repetition rate. CWE harmonics are generated by focusing the laser beam, at a maximum intensity of 8×10^{16} W cm^{-2} ($a_0 = 0.2$), on a moving disk of fused silica [17]. The harmonic frequencies contained in the beam reflected off the target surface are spectrally dispersed by a 600 grooves/mm grating onto a microchannel plate detector coupled to a fast phosphor screen, imaged by a CCD camera.

Figure 1(e) displays the experimentally measured spectral widths of CWE individual harmonic peaks, as a function of harmonic order. The harmonic width clearly increases with the harmonic order: as discussed before, this is a clear signature of an aperiodic APT. Before using these widths to determine x_ω and δ, two additional inputs are needed. First, one needs to know the temporal profile of the laser amplitude $a_0(t) \propto a_M \times f(t)$ (where a_M is the peak amplitude of the laser field), which appears in Eq. (1). In our experiment, the temporal pulse profile $f(t)$ is accurately measured using SHG FROG, and this information, together with a measurement of the pulse energy and spatial beam profile at focus, is used to determine a_M. Second, the amplitude profile of the APT, characterized by the coefficients $a(n)$, is also needed, as it determines the overall duration of the APT, which also directly influences the harmonic widths. To access this information, we measure the CWE harmonic signal as a function of the laser intensity I, using a combination of half-wave plate and polarizer to vary the incident pulse energy. The variation of the ninth harmonic intensity is plotted in Fig. 2 and can be accurately fitted by a power law I^b, with $b = 2.6$. Assuming that the time-integrated intensity dependence measured in this way can be used to calculate the temporal variation of the CWE signal, we use $a(n) = f^b(nT_L)$, with $b = 2.6$.

Under these conditions, we obtain a very good agreement between experiment and model for $\delta = \lambda_L/200$ [Fig. 1(e)], with an absolute accuracy of the order of $\lambda_L/1000$ ($\approx$1 nm). This value of δ corresponds to the time- and space-averaged plasma scale length around the peak of the laser pulse. Once the harmonic signal intensity dependence is known, δ can be obtained in a single laser shot, from measured harmonic widths such as shown in Fig. 1(e).

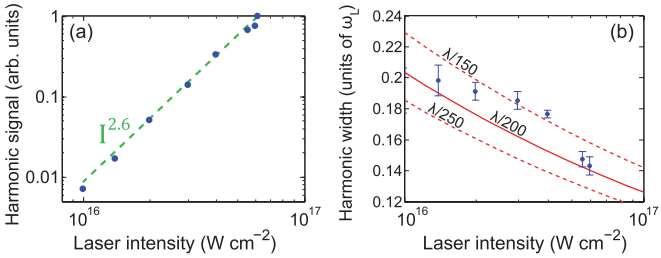

FIG. 2. (Color online) (a) Intensity of the ninth harmonic signal [filled (blue) circles] for laser intensities ranging from 10^{16} to 10^{17} W cm^{-2}, together with a power-law fit of exponent 2.6 [dashed (green) line]. (b) Width of the ninth harmonic as a function of the laser intensity, from experiment [filled (blue) circles] and from the model [(red) lines] for different plasma gradient lengths.

During the intensity scan shown in Fig. 2(a), we also observe a decrease in the ninth harmonic spectral width with increasing laser intensity [Fig. 2(b)]. This is consistent with Eq. (1) and with our previous qualitative discussion: higher field amplitudes lead to faster Brunel electrons [Figs. 1(a) and 1(b)], reducing the difference in emission time between attosecond pulses in the APT within the laser pulse and the resulting harmonic frequency chirp.

Quite remarkably, this experimental curve can also be fitted with our analytical model, using the same value of δ deduced from the measurements in Fig. 1(e). Physically, this shows that the plasma scale length does not vary significantly with laser peak intensity. This can be explained by the fact that in our experiment, according to the measured laser temporal profile, the plasma is most likely created, at most, 1 ps before the pulse peak (where the measured temporal contrast ratio is $\approx 5 \times 10^{-5}$). In this time range, the laser intensity rises very steeply in time, meaning that a change in peak intensity hardly affects the plasma formation time or, hence, the scale length δ.

In order to test the consistency and robustness of our model, we performed an additional parametric study: the harmonic width was measured as a function of the frequency chirp of the driving laser pulse (Fig. 3). As in [13], we observe a narrowing of the harmonic width with increasing positive

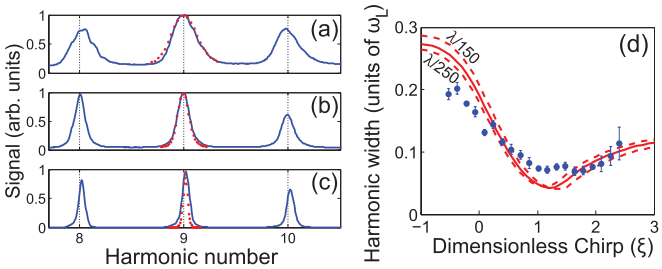

FIG. 3. (Color online) Chirp dependence of the experimental harmonic spectrum for (a) $\xi = -1$, (b) $\xi = 0$, and (c) $\xi = 1$, where ξ is the normalized quadratic spectral phase, $\xi\tau^2 = (\partial^2\phi_\omega/\partial\omega^2)_{\omega_0}$, with ϕ_ω the laser spectral phase. Dotted (red) lines show spectra obtained from the model. (d) Spectral width of the eighth harmonic as a function of the laser chirp from experiment (blue symbols) and model (red symbols) for different plasma gradient lengths: $\delta = \lambda_L/200$ (solid line); $\delta = \lambda_L/150$ and $\delta = \lambda_L/250$ (dashed lines).

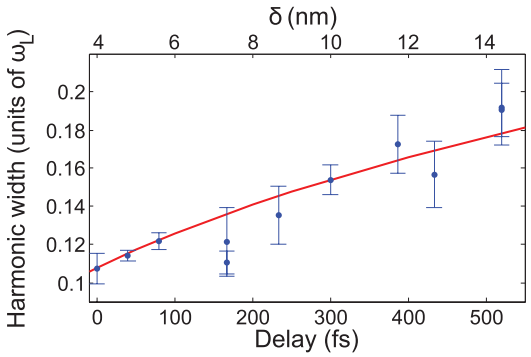

FIG. 4. (Color online) Spectral width of the eighth harmonic as a function of the delay Δt between the prepulse at 10^{15} W cm^{-2} and the probe at 9×10^{16} W cm^{-2} ($a_0 = 0.2$). The experimental results [filled (blue) circles] are fitted by the model [solid (red) lines], using an intensity dependence exponent $b = 2.6$ and a linear expansion of the plasma with $c_s = 20$ nm/ps. The upper x axis shows the values of $\delta(t) = c_s t$ used in the model for the fit.

laser chirp, down to a minimum where it compensates the intrinsic harmonic chirp (i.e., the deviation from perfect APT periodicity), and, on the contrary, a broadening for negative laser chirp. The model equations can be modified to account for the effect of the laser chirp on the attosecond pulse emission times $t_e(n)$ [16]. Using the same procedure as described before, our model quantitatively reproduces the measured trends in Fig. 3(d), with small deviations, which we attribute to high-order phase terms in the laser pulse. This dependence on laser chirp is of little use for determining the plasma density gradient since it is hardly influenced by δ. However, it does provide a validation of our model.

We now implement this measurement technique in a pump-probe scheme in order to measure the expansion velocity of a laser-induced plasma into vacuum. Experimentally, the pump pulse is generated by picking off half the initial laser pulse energy with a beam splitter and sending this portion of the beam through a delay line before loosely focusing it onto the target using a low numerical aperture lens ($f/10$). The focal spot size of this "pump" beam was thus four times larger than that of the remaining high-intensity "probe" beam. The latter is focused onto the expanding plasma, where it induces CWE, under the same conditions as before. The peak intensity of the pump pulse is estimated as 10^{15} W cm^{-2}.

The eighth harmonic spectral width measured as a function of the pump-probe delay Δt is displayed in Fig. 4. The fact that it increases with Δt is consistent with a growing gradient scale length δ associated with the expansion of the plasma triggered by the pump pulse. The red line in Fig. 4 corresponds to the results of our model, using a plasma scale length $\delta = c_s \Delta t$, a plasma expansion velocity $c_s = 20$ nm/ps, and $b = 2.6$ as before. The corresponding values of $\delta(t)$ are provided by the upper x axis in Fig. 4. This retrieved ion acoustic velocity c_s is consistent with previous measurements obtained using other techniques [7,18,19].

In conclusion, we demonstrate the first quantitative measurement of the density gradient scale length of a laser-induced plasma, using CWE spectroscopy, with nanometer-scale spatial resolution and sub-30-fs temporal resolution. This new approach probes the distance x_ω between the critical density surface and a region of highly overcritical density $N(x_\omega) \gg N_c$ within the plasma density gradient—a key difference from optical interferometric techniques. It is therefore directly sensitive to the density gradient scale length, over a range of about two orders of magnitude, between $\approx \lambda_L/200$ and $\approx \lambda_L/5$.

This work was performed using HPC resources from GENCI-CCRT/CINES (Grant No. 2011-056057). F.Q. acknowledges financial support from the European Research Council (ERC Grant Agreement No. 240013).

[1] P. Gibbon, *Short Pulse Laser Interactions with Matter* (Imperial College Press, London, 2005).
[2] A. Tarasevitch, K. Lobov, C. Wünsche, and D. von der Linde, Phys. Rev. Lett. **98**, 103902 (2007).
[3] C. Thaury and F. Quéré, J. Phys. B: At. Mol. Opt. Phys. **43**, 213001 (2010).
[4] S. S. Mao, F. Quéré, S. Guizard, X. Mao, R. E. Russo, G. Petite, and P. Martin, Appl. Phys. A **79**, 1695 (2004).
[5] J. P. Geindre, P. Audebert, A. Rousse, F. Falliès, J. C. Gauthier, A. Mysyrowicz, A. Dos Santos, G. Hamoniaux, and A. Antonetti, Opt. Lett. **19**, 1997 (1994).
[6] P. Blanc, P. Audebert, F. Falliès, J. P. Geindre, J. C. Gauthier, A. Dos Santos, A. Mysyrowicz, and A. Antonetti, J. Opt. Soc. Am. B **13**, 118 (1996).
[7] C. Quoix, G. Hamoniaux, A. Antonetti, J.-C. Gauthier, J.-P. Geindre, and P. Audebert, J. Quant. Spectrosc. Radiat. Transfer **65**, 455 (2000).
[8] F. Quéré, C. Thaury, P. Monot, S. Dobosz, Ph. Martin, J.-P. Geindre, and P. Audebert, Phys. Rev. Lett. **96**, 125004 (2006).
[9] C. Thaury, F. Quéré, J.-P. Geindre, A. Levy, T. Ceccotti, P. Monot, M. Bougeard, F. Réau, P. d'Oliveira, P. Audebert, R. Marjoribanks, and Ph. Martin, Nat. Phys. **3**, 424 (2007).
[10] B. Dromey, S. G. Rykovanov, D. Adams, R. Hörlein, Y. Nomura, D. C. Carroll, P. S. Foster, S. Kar, K. Markey, P. McKenna, D. Neely, M. Geissler, G. D. Tsakiris, and M. Zepf, Phys. Rev. Lett. **102**, 225002 (2009).
[11] F. Brunel, Phys. Rev. Lett. **59**, 52 (1987).
[12] The delay dt between the excitation of the plasma oscillations and the subsequent emission of the attosecond pulse is $dt = 2\delta(1/c + 1/v_p)$ (see Eq. (26) in [3]), where δ is the gradient scale length and v_p the Brunel electron bunch velocity. Knowing that typically $v_p \approx c/4$, this delay is of the order of $T_L/20 \approx 120$ as for $\delta \approx \lambda_L/200$.
[13] F. Quéré, C. Thaury, J-P. Geindre, G. Bonnaud, P. Monot, and Ph. Martin, Phys. Rev. Lett. **100**, 095004 (2008).
[14] C. Thaury, H. George, F. Quéré, R. Loch, J.-P. Geindre, P. Monot, and Ph. Martin, Nat. Phys. **4**, 631 (2008).

[15] A. Borot, A. Malvache, X. Chen, A. Jullien, J.-P. Geindre, P. Audebert, G. Mourou, F. Quéré, and R. Lopez-Martens, Nat. Phys. **8**, 416 (2012).

[16] See Supplemental Material at http://link.aps.org/supplemental/10.1103/PhysRevE.87.035101 for the derivation of the analytical formula for the CWE attosecond pulse emission time and its validation using particle-in-cell code.

[17] A. Borot, A. Malvache, X. Chen, D. Douillet, G. Iaquianiello, T. Lefrou, P. Audebert, J.-P. Geindre, G. Mourou, F. Quéré, and R. Lopez-Martens, Opt. Lett. **36**, 1461 (2011).

[18] B. Vu, A. Szoke, and O. Landen, Phys. Rev. Lett. **72**, 3823 (1994).

[19] G. Doumy, F. Quéré, O. Gobert, M. Perdrix, Ph. Martin, P. Audebert, J. C. Gauthier, J.-P. Geindre, and T. Wittmann, Phys. Rev. E **69**, 026402 (2004).